ARTICLE

BIOTECHNOLOGY and BIOENGINEERING

Alleviating Product Inhibition in Cellulase Enzyme Cel7A

Meera E. Atreya,[1,2] Kathryn L. Strobel,[2,3] Douglas S. Clark[2,3]

[1]Department of Chemistry, Chemical Biology Graduate Program, University of California, Berkeley 94720, California

[2]Energy Biosciences Institute, University of California, Berkeley 94720, California

[3]Department of Chemical and Biomolecular Engineering, University of California, Berkeley 94720, California; telephone: 510-642-2408; fax: 510-643-1228; e-mail: clark@berkeley.edu

ABSTRACT: Enzymes that degrade cellulose into glucose are one of the most expensive components of processes for converting cellulosic biomass to fuels and chemicals. Cellulase enzyme Cel7A is the most abundant enzyme naturally employed by fungi to depolymerize cellulose, and like other cellulases is inhibited by its product, cellobiose. There is thus great economic incentive for minimizing the detrimental effects of product inhibition on Cel7A. In this work, we experimentally generated 10 previously proposed site-directed mutant Cel7A enzymes expected to have reduced cellobiose binding energies (the majority of mutations were to alanine). We then tested their resilience to cellobiose as well as their hydrolytic activities on microcrystalline cellulose. Although every mutation tested conferred reduced product inhibition (and abolished it for some), our results confirm a trade-off between Cel7A tolerance to cellobiose and enzymatic activity: Reduced product inhibition was accompanied by lower overall enzymatic activity on crystalline cellulose for the mutants tested. The tempering effect of mutations on inhibition was nearly constant despite relatively large differences in activities of the mutants. Our work identifies an amino acid in the Cel7A product binding site of interest for further mutational studies, and highlights both the challenge and the opportunity of enzyme engineering toward improving product tolerance in Cel7A.

Biotechnol. Bioeng. 2016;113: 330–338.

KEYWORDS: cellulosic biofuels; cellulase; glycoside hydrolase family 7; Cel7A; cellobiohydrolase I (CBH1); product inhibition; cellobiose

Corresponding to: D.S. Clark

Contract grant sponsor: Energy Biosciences Institute

Received 6 July 2015; Revision received 19 August 2015; Accepted 21 August 2015

Accepted manuscript online 24 August 2015;

Article first published online 10 September 2015 in Wiley Online Library (http://onlinelibrary.wiley.com/doi/10.1002/bit.25809/abstract).

DOI 10.1002/bit.25809

Introduction

Biofuels represent one of many important renewable energy alternatives to fossil fuels with the potential to decrease anthropogenic effects on climate change. Cellulosic biofuels derive energy from chemical bonds stored by plants in the form of cellulose, a polymer of glucose, and a primary structural component of plant cell walls (Somerville et al., 2004). Cellulose-rich biomass can be produced with fewer inputs than first-generation biofuel crops, such as starch-rich corn; however, cellulose is difficult to break down (Dinan, 2014). Once cellulose is depolymerized into glucose, the sugar can be microbially or chemically transformed into fuels and chemicals such as ethanol, butanol, or other gasoline, jet fuel, and diesel alternatives.

While cellulose is abundant, accessing the sugar within is challenging. To biochemically degrade biomass, several enzymes work in concert, the most abundant of which is cellulase enzyme Cel7A (Payne et al., 2015). Cel7A cellobiohydrolase enzymes depolymerize cellulose into its fundamental repeating unit of two glucose molecules—cellobiose. These enzymes suffer from inhibition by this product, which lingers in the enzymes' active sites and thus delays their catalytic cycles (Silveira and Skaf, 2015). Cellobiose accumulates over the course of a reaction unless removed by an enzyme such as β-glucosidase, which cleaves cellobiose yielding two glucose molecules (Payne et al., 2015). Cel7A experiences mixed inhibition by cellobiose; the molecule can both competitively compete with a cellulose chain for binding in the substrate-binding sites as well as noncompetitively inhibit the enzyme by retarding processive motion as a result of persisting in the product-binding site (Jalak et al., 2012; Payne et al., 2015). Measurements on crystalline cellulose show that Cel7A loses half of its activity in the presence of cellobiose concentrations on the order of 2.6 mM (Teugjas and Väljamäe, 2013) to 19 mM (Murphy et al., 2013). Product inhibition is particularly nefarious in the enzymatic conversion of lignocellulosic biomass to glucose under the high substrate loadings required for commercial manufacture of biofuels, and represents a barrier to achieving the high product yields necessary for an efficient process (Bu et al., 2012; Payne et al., 2015). Unfortunately, addressing this issue with the product inhibition-relieving enzyme β-glucosidase alone is not a

comprehensive solution. Beta-glucosidase activity is limited by its own product inhibition from glucose, as well as by gluconic acid (generated by lytic polysaccharide monooxygenase (LPMO) activity) (Payne et al., 2015).

Enzymes are one of the most expensive components of a biochemical cellulosic biofuels process (Klein-Marcuschamer et al., 2012). Therefore, improving the efficiency of Cel7A by ameliorating product inhibition may result in a lower enzyme requirement for the process and consequently a cheaper renewable fuel that is more cost-competitive with fossil fuels. To this end, several research groups have investigated ways to make Cel7A enzymes less prone to cellobiose inhibition. The prevailing strategy to mitigate product inhibition has been to perturb the binding of cellobiose in the enzyme active site via site-directed mutagenesis of the residues most responsible for this interaction (Hanson et al., 2014; Payne et al., 2015; Silveira and Skaf, 2015). Mutations in *Trichoderma reesei* (*Hypocrea jecorina*) Cel7A (*Tr*Cel7A) residues R251 and R394 reportedly resulted in reduced product inhibition (Hanson et al., 2014). A quintuple *Tr*Cel7A mutant (E223S/A224H/L225V/T226A/D262G) designed in 2001 to alter the pH optimum was similarly found to both relieve cellobiose inhibition and diminish overall cellulase activity (Becker et al., 2001). More recently, computational point mutation studies in the same enzyme found that mutating residues R251, D259, D262, W376, or Y381 to alanine significantly weakened the calculated binding of cellobiose in the enzyme (Bu et al., 2011; Payne et al., 2015). However, for many of these residues, no experimental evidence verifying this has ever been demonstrated.

Recent molecular dynamics (MD) simulations performed by Silveira and Skaf computationally investigated the effects of various Cel7A mutations on cellobiose binding, as well as any induced structural perturbations to the enzyme (Silveira and Skaf, 2015). These simulations built upon previous calculations (Bu et al., 2011) and together point to a handful of mutations predicted to disrupt cellobiose binding affinity (Silveira and Skaf, 2015). The aim of our study, was to produce a Cel7A variant with reduced cellobiose inhibition. We experimentally generated mutants identified by MD simulations (Silveira and Skaf, 2015) and evaluated their ability to hydrolyze microcrystalline cellulose in the presence of cellobiose.

Materials and Methods

Selection of Cel7A Mutations

Cel7A mutations for experimental analyses were selected based on computational studies (Bu et al., 2011; Silveira and Skaf, 2015) (T226A, R251A, D259A, D262A, R267A, W376A, Y381A, R394A) and an industrial patent (Hanson et al., 2014) (R251K and R251K + R394A). Tris-HCl cellobiose binding site mutations were mapped onto the *Talaromyces emersonii* Cel7A (*Te*Cel7A) enzyme. Protein sequences of *Tr*Cel7A (Uniprot accession number: P62694) and *Te*Cel7A (Uniprot accession number: Q8TFL9) were aligned using the ExPASy Bioinformatics Resource Portal local similarity program alignment tool (Supplemental Fig. S1). Ten mutations were mapped as shown in Table I.

Construction of *Te*Cel7A Enzymes

*Te*Cel7A variants were generated in yeast expression vector pCu424 (Labbé and Thiele, 1999). Because *Te*Cel7A does not naturally contain a carbohydrate binding module (CBM), the CBM from *Agaricus bisporus* (Uniprot accession number: Q92400) was appended to the catalytic domain using a short, flexible linker from *Acremonium thermophilum* (Uniprot accession number: A7WNT9) as described previously (Dana et al., 2012). Inclusion of the native signal sequence allowed for secreted enzyme expression and enabled the mature form of the protein to carry the proper N-terminal pyroglutamate following signal sequence cleavage (Dana et al., 2014). DNA and protein sequences encoding the wild-type *Te*Cel7A enzyme (with added linker and CBM) are detailed in Supplemental Figure S2.

Site-directed mutagenesis was performed by PCR amplification of the pCu424 *Te*Cel7A DNA construct using overlapping primers to replace wild-type codons with those encoding the desired amino acid substitutions (Supplemental Table SI). Replacement codons were selected based on their natural abundance in *S. cerevisiae*. A negative control sample lacking any cellulase gene was also generated by removing the DNA encoding the catalytic domain, linker, and CBM domain from the expression vector. Amplification reactions were verified using agarose gel electrophoresis. Methylated template DNA was digested overnight at 37°C by restriction endonuclease DpnI (NEB, Ipswich, MA). All resulting plasmids were independently cloned into XL1-Blue *E. coli* cells (Agilent Technologies, Santa Clara, CA) followed by overnight culture growth at 37°C in Lysogeny Broth (LB) media containing 65 mg/L carbenicillin antibiotic. The amplified vector DNA from the resulting cultures was purified using Quiagen Miniprep kits (Quiagen, Limburg, Netherlands) and thereafter sequenced to verify successful mutagenesis.

Expression of *Te*Cel7A Enzymes

Control sample and point-mutant pCU424 *Te*Cel7A DNA were individually transformed using the lithium acetate method (Daniel and Woods, 2002) into the enzyme production host organism, *S. cerevisiae* strain YVH10Δ*PMR1* (a strain which limits protein hyperglycosylation) (Dana et al., 2012). Cells were spread onto selective plates containing 1.5% agar and synthetic complete medium lacking tryptophan (SC-Trp) and incubated for three days at 30°C. Liquid cultures of 100 mL SC-Trp for each variant were inoculated with plate colonies and grown overnight at 30°C with shaking at 220 rpm before being used, in turn, to inoculate 2 L

Table I. Amino acid residues mapped from *T. reesei* Cel7A to *T. emersonii* Cel7A.

Enzyme	Mutation									
*Tr*Cel7A	R251K/R394A	Y381A	D262A	W376A	T226A	R394A	R251A	D259A	R267A	R251K
*Te*Cel7A	R248K/R398A	Y385A	D259A	W380A	T223A	R398A	R248A	D256A	R264A	R248K

cultures grown for three days under the same conditions. *Te*Cel7A protein expression was then induced by pelleting the cells via centrifugation at 4,000*g* for 15 min and resuspending them in yeast peptone dextrose (YPD) medium supplemented with 500 μM copper sulfate. The induced cultures were grown for an additional three days at 25°C with shaking at 220 rpm.

Purification of *Te*Cel7A Enzymes

Following protein expression, cultures were centrifuged at 4,000*g* for 15 min to clarify the supernatants containing the *Te*Cel7A enzymes. Two liters of yeast culture supernatant for each variant were subsequently filtered (to remove residual cells) before being concentrated and buffer exchanged via tangential flow filtration (TFF) into 20 mM Tris-HCl, pH 7.

Proteins were purified using fast protein liquid chromatography (FPLC) over 5 mL HiTrap Q HP columns (GE Healthcare, Little Chalfont, UK) using running buffer 20 mM Tris-HCl, pH 7, and elution buffer of the same with the addition of 1 M sodium chloride. Gradients of 0–25% elution buffer (0–0.25 M sodium chloride) over 85 mL followed by 25–50% elution buffer (0.25–0.5 M sodium chloride) over 35 mL were used to separate supernatant proteins.

FPLC fractions were analyzed for cellulase activity using 4-methylumbelliferyl-β-D-cellobioside (MUCell), a fluorescent substrate mimic. Twenty microliters of each FPLC fraction sample was mixed with 80 μL of 1.25 mM MUCell in 50 mM sodium acetate, pH 5 and heated for 10 min at 50°C. Reactions were stopped by boiling at 98°C for 2 min and prepared for analysis by the addition of 10 μL of 1 M sodium hydroxide. Fluorescence was measured using a multiwell plate reader with an excitation wavelength of 365 nm and an emission wavelength of 445 nm. Active fractions were analyzed for purity using SDS-PAGE, and those containing uncontaminated *Te*Cel7A enzymes (running at ~75 kDa) were combined. Samples were concentrated and buffer exchanged into 50 mM sodium acetate, pH 5 using 30 k MWCO Vivaspin 15 Turbo centrifugal concentrators (Sartorius, Concord, CA). Enzyme concentrations were normalized to $A_{280} = 1$, or approximately 13.35 μM, and were of single-band purity (Supplemental Fig. S3).

Activity Assays

Assays to measure activity and inhibition of purified enzymes on cellulose were performed in 96-well PCR plates with 10 mg/mL Avicel PH-101 (Sigma, St. Louis, MO) substrate and 1.33 μM purified *Te*Cel7A enzyme in 50 mM sodium acetate, pH 5. Three sets of experiments were performed: (i) without β-glucosidase (150 μL reaction volumes, performed in triplicate); (ii) with β-glucosidase (150 μL reaction volumes, performed in triplicate); and (iii) with thiocellobiose and β-glucosidase (75 μL reaction volumes, performed in duplicate). Reactions including β-glucosidase contained 0.016 g/L β-glucosidase (cellobiase) from *Aspergillus niger* (Novozyme 188, Novozymes, Bagsvaerd, Denmark). Reactions including thiocellobiose contained 4.39 g/L thiocellobiose (Sigma, St. Louis, MO). All experiments were incubated for 60 h at 60°C with constant rotational mixing followed by boiling for 5 min at 95°C to stop the reactions.

Activity Assay Analysis

To quantify the cellobiose and glucose concentrations in the reactions, samples were filtered through 96-well filter plates with 0.45 μm polypropylene membranes (Seahorse Bioscience, North Bellerica, MA) and analyzed in 96-conical well plates sealed by aluminum tape using a 1200 series high-pressure liquid chromatography (HPLC) system (Agilent Technologies, Santa Clara, CA) consisting of an autosampler with tray cooling, binary pump, degasser, thermostated column compartment, diode array detector (DAD), and refractive index detector (RI) connected in series. The supernatant (20 μL) was injected onto a 100 × 7.8 mm (length × inner diameter) Rezex™ RFQ-Fast Acid H^+ guard column (Phenomenex, Torrance, CA) with 8 μm particle size, 8% cross-linkage equipped with a SecurityGuard™ Standard Carbo H^+ (Phenomenex) column cartridge. Compounds were eluted at 55°C at a flow rate of 1.0 mL using a mobile phase of 5 mM sulfuric acid. Quantification was performed by external calibration with a set of cellobiose and glucose solutions in the ranges of 0.08–10 mg/mL and 0.15–20 mg/mL, respectively.

Data presented represents average values of experiments (controls subtracted) with standard error ($n = 3$ for experiments with and without β-glucosidase, $n = 2$ for experiments with thiocellobiose). Reported ratio values are quotients of averages with propagated standard error from the two measurements. Percentage changes in enzymatic activity and cellobiose tolerance (ratio of activities without and with β-glucosidase present), relative to the wild-type enzyme, were calculated by dividing the differences between mutant and wild-type values by the wild-type values.

Isothermal Titration Calorimetry

Isothermal titration calorimetry (ITC) was carried out using a TA Instruments Nano-ITC (New Castle, DE). Protein and ligands were prepared by buffer exchanging protein samples into 50 mM sodium acetate, pH 5.0, using centrifugal concentrators, and dissolving ligands in the final flow-through solution from the buffer exchange process. This insured low background during titrations due to heterogeneous buffer compositions. All experiments were conducted at 10°C using a stirring speed of 250 rpm and 25 μM Cel7A in the sample cell. Injections of 0.65–4 mM cellobiose (depending on the mutant being studied) were made every 400 s until saturation was reached. Blank titrations were performed without enzyme to control for heats of dilution and mixing. The blank titrations were subtracted from the experimental titrations prior to data analysis. Binding parameters were determined by fitting the data using TA Instruments NanoAnalyze software to an independent binding site model. Reported values are the average and standard deviation from three or two separate experiments for the *Te*Cel7A wild-type and Y385A mutant enzymes, respectively.

Results and Discussion

Recent molecular dynamics (MD) simulations (Silveira and Skaf, 2015) identified several *T. reesei* Cel7A mutations (many of which were revealed previously (Becker et al., 2001; Bu et al., 2011; Hanson et al., 2014)) predicted to reduce product inhibition. Seven of the

eight residues selected in the MD studies for mutation to alanine interact with cellobiose at an energy below −5 kcal/mol, indicating that each residue significantly contributes to cellobiose affinity (Silveira and Skaf, 2015). We experimentally generated ten Cel7A mutants, chosen based on MD work in the literature and an industrial patent, and examined their activities under various inhibiting and non-inhibiting conditions. We mapped the mutations simulated for *T. reesei* Cel7A onto a homologous Cel7A catalytic domain from *T. emersonii* (Table I). Due to the structural similarity and highly conserved active sites of these proteins (Fig. 1), we expected mutations calculated to relieve product inhibition in *Tr*Cel7A to effect similar outcomes in *Te*Cel7A. Although *T. reesei* is currently the industrial standard for cellulase production, we chose to work with *Te*Cel7A because it is more thermotolerant than *Tr*Cel7A (Payne et al., 2015) and expresses at higher titers in the laboratory host production organism *Saccharomyces cerevisiae* (data not shown). Thermostable cellulases are of interest industrially as high-temperature cellulose hydrolysis decreases the risk of contamination and enables a greater solid substrate loading due to reduced slurry viscosity (Gericke et al., 2009). Thus, *Te*Cel7A is of substantial relevance to the field and has the additional benefit of facile heterologous expression in *S. cerevisiae* (Dana et al., 2012).

Enzyme product inhibition was estimated by comparing enzymatic hydrolysis of cellulose under inhibiting conditions to hydrolysis when the enzyme was minimally inhibited. Although *Te*Cel7A is thermotolerant, reactions were performed at 60°C in order to preserve the effectiveness of the β-glucosidase enzyme used. At 70°C, all *Te*Cel7A enzymes were indeed active, but little difference was observed between samples with and without β-glucosidase (Supplemental Fig. S4). This is consistent with a β-glucosidase enzyme that is inactive at this temperature.

Enzymatic hydrolysis of Avicel by Cel7A variants with and without β-glucosidase present is compared in Figure 2, and the corresponding cellobiose and glucose concentrations (and their ratios) are listed in Supplemental Table II. In reactions containing β-glucosidase, the Cel7A enzymes were negligibly inhibited by cellobiose, as any cellobiose generated was quickly cleaved to glucose by β-glucosidase (no more than 0.02 g/L of cellobiose was measured in these experiments). Reactions lacking β-glucosidase, on the other hand, experienced varying inhibitor concentrations as a result of cellobiose accumulating over the course of hydrolysis. The final cellobiose concentrations in reactions without β-glucosidase ranged from 0.20 g/L (0.58 mM, for the least active mutant, *Te*Cel7A W380A) to 0.61 g/L (1.8 mM, for the wild-type *Te*Cel7A enzyme). All assays had 10 g/L Avicel; therefore, the maximum conversion reached was approximately 9%. These low conversions were expected, given the relatively low enzyme loading and the absence of endoglucanases and other synergistic enzymes.

Enzyme tolerance to the inhibitor cellobiose can be estimated by comparing the extent of hydrolysis under inhibiting conditions (without β-glucosidase) to that when inhibition is alleviated (with β-glucosidase) (Hanson et al., 2014). Accordingly, a ratio of one represents the best-case scenario, whereby an enzyme retains 100% of its uninhibited activity in the presence of cellobiose. As predicted (Bu et al., 2011; Hanson et al., 2014; Silveira and Skaf, 2015),

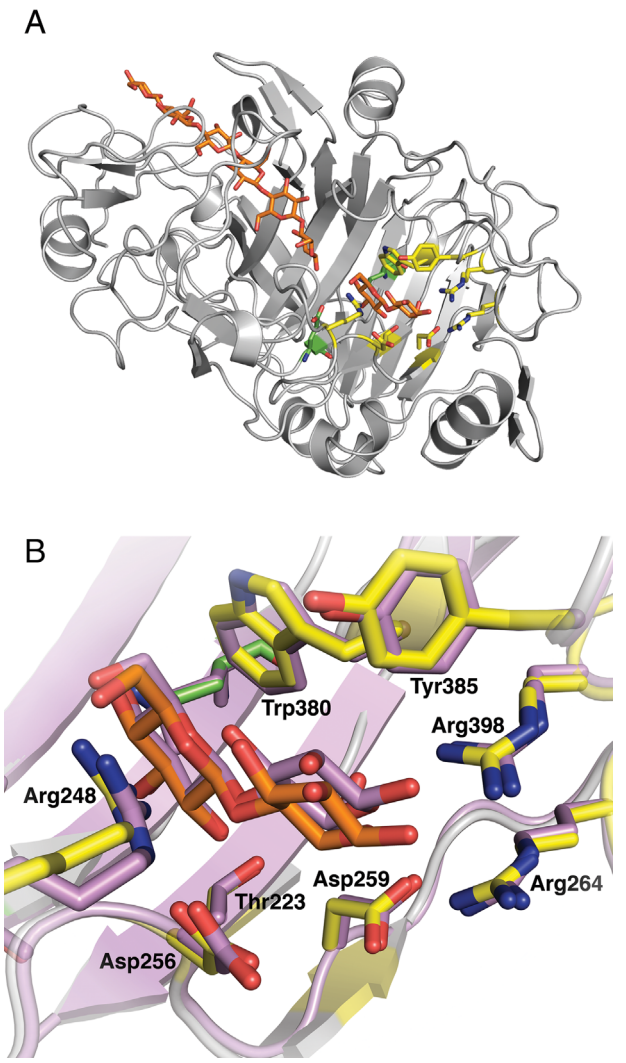

Figure 1. (**A**) *T. reesei* Cel7A, PDB: 7CEL (gray) bound to a cellulose substrate chain and product cellobiose (orange). Amino acid residues selected for site-directed mutagenesis in the enzymes' binding tunnel are highlighted in yellow and catalytic residues are shown in green. (**B**) A close-up of the cellobiose product binding site showing the alignment of *T. reesei* Cel7A (gray and yellow, PDB: 7CEL) with *T. emersonii* Cel7A (violet, PDB: 3PFX). The cellobiose from the *T. reesei* crystal structure is shown in orange and one from *T. emersonii* in violet. Residue numbering corresponds to the *T. emersonii* Cel7A enzyme.

compared to the wild-type, every mutation tested improved the enzyme's tolerance to cellobiose (Fig. 2B); however, in the conditions examined, the wild-type *Te*Cel7A was more active than any mutant toward depolymerizing crystalline cellulose (Fig. 2A). While the wild-type *Te*Cel7A enzyme retained only 72% of its activity under inhibiting conditions, mutants Y385A, D259A, and W380A, for example, retained 86%, 96%, and 98%, respectively, of their activities when inhibited. Double mutant R248K/R398A and single mutant R248A, in particular, exhibited no measurable loss of activity under these inhibiting conditions. BP Biofuels similarly found the corresponding two mutants in *Tr*Cel7A to behave favorably with respect to cellobiose tolerance (Hanson et al., 2014).

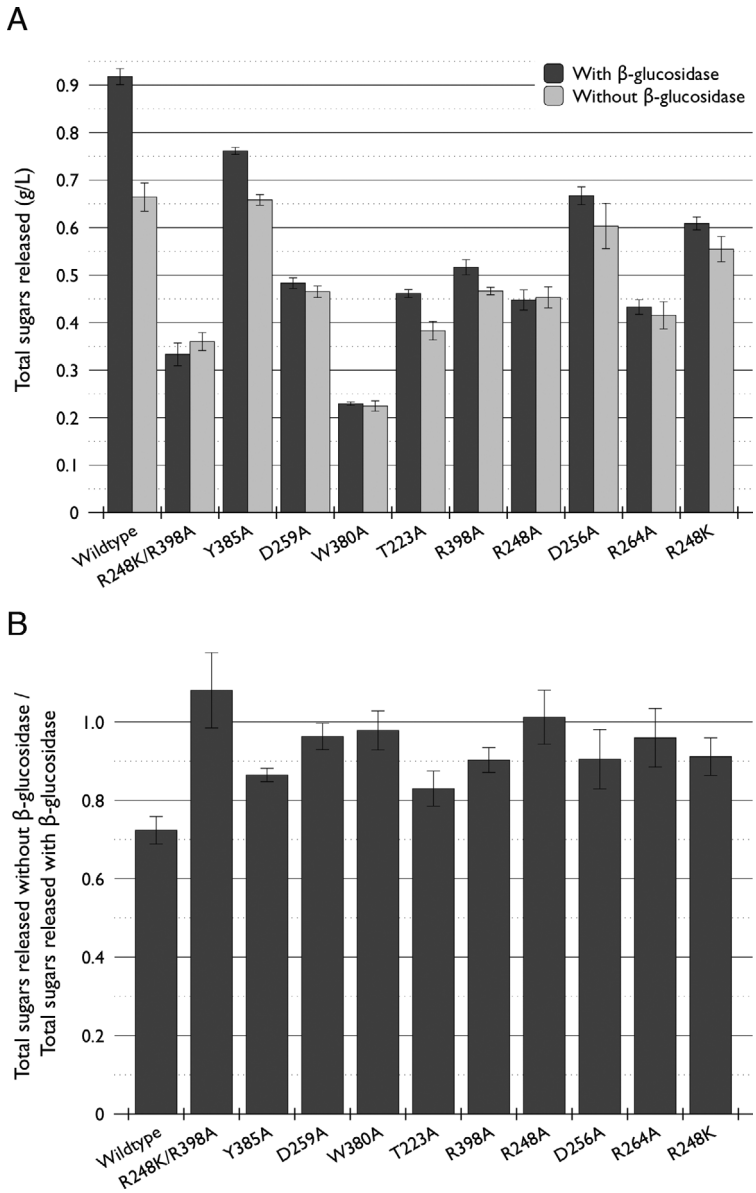

Figure 2. (**A**) Total sugars (cellobiose + glucose, g/L) released from Avicel hydrolysis by *Te*Cel7A enzymes under minimally inhibiting ("with β-glucosidase") or inhibiting ("without β-glucosidase") conditions after 60 h at 60°C. Error bars represent standard error ($n = 3$). (**B**) Enzyme tolerance to cellobiose, based on the ratio of activities of *Te*Cel7A enzymes under inhibiting conditions to activities under minimally inhibiting conditions. Error bars represent propagated standard error.

Enzyme tolerance to cellobiose was also studied under conditions providing equivalent inhibition across all samples using the cellobiose mimic, thiocellobiose. Thiocellobiose, while chemically very similar to cellobiose, is not cleaved by β-glucosidase; its concentration therefore remained constant throughout the hydrolysis reactions. Enzymatic activities under inhibition by 4.39 g/L thiocellobiose (Fig. 3) corroborate results from hydrolysis under inhibition by auto-generated cellobiose (Fig. 2A, "without β-glucosidase"). The wild-type *Te*Cel7A was again the most productive enzyme assayed. Thus, the mutations suggested by MD simulations (Silveira and Skaf, 2015) did alleviate product inhibition (Fig. 2B), but always at the expense of activity under the conditions tested.

Of the *Te*Cel7A variants examined, a few mutants were of particular interest, including Y385A and R248K. Relative to that of the wild-type enzyme, the Y385A mutant demonstrated an improved tolerance to cellobiose (+19% compared to the wild-type, Fig. 2B) with the least loss in activity (−17% uninhibited, −1% inhibited compared to the wild-type, Fig. 2A). The R248K mutant also exhibited improved cellobiose tolerance (+26%), but a greater loss in activity relative to the wild-type enzyme (−34% uninhibited, −16% inhibited). Interestingly, MD simulations predicted that the residues corresponding to *Te*Cel7A R248 and Y385 (displayed in yellow in Fig. 4) may interact to form a closed, tunnel-like conformation. This conformation, inaccessible until after hydrolysis of the carbohydrate substrate chain, may obstruct

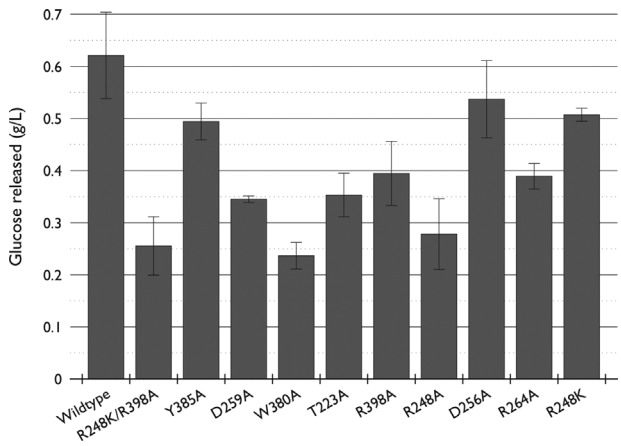

Figure 3. Glucose released from Avicel hydrolysis by *Te*Cel7A enzymes under conditions of equivalent inhibition by thiocellobiose after 60 h at 60°C. Error bars represent standard error ($n = 2$).

cellobiose product release (Silveira and Skaf, 2015). The reduction we observed in cellobiose inhibition may thus be a consequence of removing the protein's ability to adopt this occluding conformation. Indeed, MD calculations predicted *Tr*Cel7A mutant Y381A (*Te*Cel7A Y385A) to have a substantial impact on cellobiose binding free energy, shifting it from approximately −14 kcal/mol to −9 kcal/mol (Bu et al., 2011; Silveira and Skaf, 2015).

Additionally, as the guanido group of *Tr*Cel7A R251 (*Te*Cel7A R248) is known to make two hydrogen bonds with the sugar at the +1 subsite (Payne et al., 2015), it was unsurprising that eliminating those interactions in *Te*Cel7A mutant R248A reduced the enzyme's cellobiose sensitivity. However, despite its favorable inhibited: uninhibited enzymatic activity ratio (Fig. 2B), the mutant's activity relative to the wild-type suffered more than that of R248K (−51% versus −34% uninhibited, and −32% versus −16% inhibited, respectively, Fig. 2A). Indeed, MD simulations concluded that the product binding site (of the *Tr*Cel7A equivalent of *Te*Cel7A mutant R248A) loses its structural integrity due to the disruption of a conserved salt bridge with D256 (Silveira and Skaf, 2015). Perhaps the less drastic substitution of lysine for arginine (instead of alanine) in *Te*Cel7A residue 248 allowed the enzyme to maintain the salt bridge with D256 (as well as some electrostatic interactions with the sugar), while disfavoring the protein structural change occluding cellobiose release (resulting from the interaction of amino acids 248 and 385).

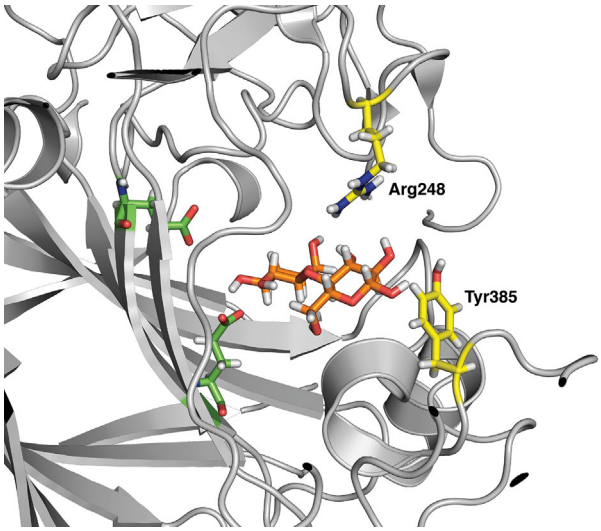

Figure 4. Cellobiose (orange) occupying the product binding sites +1 and +2 of the binding tunnel of *Te*Cel7A. Residues R248 and Y385 (shown in yellow) may interact to form a closed, tunnel-like conformation obstructing product release. Catalytic residues are shown in green.

The cellobiose affinities of the *Te*Cel7A wild-type enzyme and Y385A mutant were quantified using ITC experiments. The dissociation constant, enthalpy, and stoichiometry measured are recorded in Table II. Representative thermograms are shown in Supplemental Figure S5. Both the wild-type and Y385A mutant bound cellobiose exothermically in an equimolar ratio, consistent with *T. reesei* and *T. emersonii* Cel7A crystal structures showing one cellobiose bound per protein (Divne et al., 1998). The dissociation constant, Kd, is approximately five-fold higher for the Y385A mutant than for the wild-type enzyme, while the heat of binding is within error of the wild-type enzyme. This indicates that the difference in affinity between the two is entirely due to entropy. In both the *T. emersonii* and *T. reesei* Cel7A crystal structures, Y385 (Y381 in *T. reesei*) is not predicted to be in polar contact with cellobiose, signifying that this residue does not hydrogen bond to cellobiose. Mutating this amino acid to alanine is therefore not expected to change the heat of binding. The higher dissociation constant of the mutant confirms that this enzyme is less inhibited by cellobiose due to reduced binding affinity. The weak affinity of the Y385A mutant for cellobiose is near the detection limit for ITC. ITC experiments were attempted with D259A and W380A; however, no signal could be detected due to insufficient cellobiose affinity.

The mutant exhibiting the largest reduction in activity relative to the wild-type *Te*Cel7A enzyme was W380A (−75% uninhibited, −66% inhibited, Fig. 2A). This residue and three other aromatic amino acids directly interact with the cellulose chain and remain in place during substrate translocation, stacking with the glucosyl moieties of the substrate polymer bound in the +1, −2, −4, and −7 subsites (Knott et al., 2014; Nakamura et al., 2013; Payne et al., 2015). These interactions between aromatic amino acids and the carbohydrate are considered important for enzyme processivity (Knott et al., 2014). In fact, mutations of these residues are known to handicap processivity and thus hydrolytic activity on crystalline cellulose substrates (while increasing activity on amorphous and soluble substrates) (Knott et al., 2014). Our results are consistent

Table II. Thermodynamic parameters for the binding of cellobiose to *Te*Cel7A wild-type and Y385A enzymes.

Parameter	Wildtype	Y385A
Dissociation constant (Kd, μM)	17.9 ± 0.9	95 ± 6
Heat of binding (ΔH, kJ/mol)	−20 ± 1	−18 ± 2
Stoichiometry (n)	1.05 ± 0.01	1.01 ± 0.03

with these findings. In addition, MD simulations predicted this mutation to have a significant impact on cellobiose binding affinity, changing the calculated absolute binding free energy by roughly 7 kcal/mol (Bu et al., 2011; Silveira and Skaf, 2015). Indeed, the corresponding interaction was too weak to measure by ITC. The low affinity of cellobiose for the mutant resulted in the molecule having little inhibitory effect on the enzyme; under inhibiting conditions, the W380A mutant retained 98% of its uninhibited activity (Fig. 2B).

Mutant Y385A was arguably the best of those tested in that it was the most active relative to the wild-type enzyme (Fig. 2A) while still ameliorating product inhibition (Fig. 2B). Isothermal titration calorimetry experiments confirmed that this mutant decreased, but did not eliminate, cellobiose binding affinity to the enzyme (Table II). On the other hand, product binding was more substantially weakened in mutant W380A, for example, to the point of being undetectable by ITC. While W380A showed virtually no sensitivity to cellobiose, the hydrolytic activity of this mutant was the lowest measured. Likewise, combining mutations R248K and R398A resulted in a double mutant with an increased tolerance to cellobiose but reduced hydrolytic activity compared to the single mutants.

A loss of enzyme effectiveness in hydrolyzing cellulose, relative to the wild-type enzyme, was also expected for mutants D256A and R398A. Due almost exclusively to these two amino acids, the foremost glucose unit of the cellulose chain (occupying the +2 subsite of the enzyme's active site) forms more hydrogen bonds with Cel7A than does any other sugar of the carbohydrate substrate chain. These strong hydrogen bonds between the leading glycosyl ring and *Tr*Cel7A, D259, and R394 (*Te*Cel7A, D256, and R398 respectively) stabilize the end point of processive motion (Knott et al., 2014). Naturally, disrupting these interactions would lead to decreased hydrolysis activity on solid cellulosic substrates, as we observed experimentally for these enzyme mutants. Additionally, recent MD calculations found that the *Tr*Cel7A D259A (*Te*Cel7A D256A) mutation disrupts a salt bridge with *Tr*Cel7A R251 (*Te*Cel7A R248), as discussed above for the *Te*Cel7A R248A mutant (Silveira and Skaf, 2015). Finally, unintentional structural perturbations outside of the active site may contribute to decreased activity in the *Te*Cel7A mutants. The substrate entrance region of the protein, in particular, was computationally observed to be structurally the most sensitive part of the enzyme to mutations in the product binding site (Silveira and Skaf, 2015).

Energy calculations point to a direct link between the binding free energy of cello-oligosaccharides and enzyme processivity (Mulakala and Reilly, 2005; Payne et al., 2013). The notable affinity of Cel7A's product binding site for carbohydrate chains is believed to provide the thermodynamic driving force for processivity of the enzyme along the cellulose strand (Knott et al., 2014). In fact, cellobiose has been calculated to be 11.2–14.4 kcal/mol more stable in the product binding site of the enzyme than in free solution (Bu et al., 2011). Within the active site, computational studies have quantitatively demonstrated that a cellulose chain binds more tightly to product binding sites than it does to reactant sites of *Tr*Cel7A (Bu et al., 2011; Payne et al., 2013). Recent calorimetry experiments, corroborated this conclusion that substrate affinity is highest in the +1 and +2 (product) subsites of the enzyme's active tunnel (Colussi et al., 2015). This strong, preferential binding of the product likely contributes significantly to both the processivity of cellobiohydrolases and to their inhibition by cellobiose (Payne et al., 2013). The amino acids primarily responsible for the strong binding of the leading glycosyl residue of the cellulose chain D259 and R394 in *Tr*Cel7A (D256 and R398, respectively, in *Te*Cel7A) are conserved (Payne et al., 2015). As a result, it is unsurprising that we observed a trade-off between reduced sensitivity to inhibition by cellobiose, and overall enzyme activity on crystalline cellulose, where tight binding of the product may in fact drive processive motion along a cellulose chain.

In a hydrolysis reaction, inhibition by cellobiose is predominantly a concern for cellobiohydrolases like Cel7A (with a closed substrate binding tunnel) as opposed to endoglucanases (having an open binding cleft facilitating dissociation of this product from the active site) (Bu et al., 2012; Murphy et al., 2013; Payne et al., 2015; Teugjas and Väljamäe, 2013). Complexation with glucan chains, enzyme glycosylation (during stereochemistry-retaining glucan hydrolysis), product expulsion, processive motion along the substrate chain, and dissociation have each been hypothesized to be the rate-limiting step for Cel7A-catalyzed hydrolysis of cellulose (Fox et al., 2011; Kuusk et al., 2015; Payne et al., 2015). Product expulsion (and thus cellobiose inhibition), however, has been experimentally rejected as the cause of the observed rate retardation in enzymatic hydrolysis (Jalak et al., 2012). Regardless of the rate-limiting step, alleviating product inhibition of Cel7A should improve cellulose hydrolysis rates by increasing the concentration of catalytically viable Cel7A (Fox et al., 2011), provided the beneficial effect is not outweighed by an accompanying loss of catalytic activity.

We found that mutations identified using computational methods could be mapped between enzymes with highly-conserved active sites (and nearly identical three-dimensional structures, Fig. 1B) to effect the desired decreases in product inhibition in the homolog enzyme. In addition, data published by BP Biofuels on product-tolerant *Tr*Cel7A mutants (Hanson et al., 2014) were similar to data from our experiments with three corresponding mutants in *Te*Cel7A (R248K/R398A, R248K, and R398A). While *Tr*Cel7A is the industrial standard, the enzyme can be problematic for mutational studies due to both the complicated native *T. reesei* expression system and relatively intractable heterologous expression of *Tr*Cel7A in laboratory hosts commonly used for high-throughput experiments (Payne et al., 2015). For studies on product tolerance, our work suggests that the *S. cerevisiae*-produced *Te*Cel7A serves as a suitable replacement for *Tr*Cel7A that is both facile to work with and more thermostable. In principle, mutations of interest generated in *Te*Cel7A could be mapped back to *Tr*Cel7A for industrial production.

Considering all the mutants together provides insights into how mutations in the product binding site of Cel7A affect both the enzyme's sensitivity to inhibition by cellobiose as well as its overall hydrolytic activity on solid cellulosic substrates. Figures 5 and 6 plot the extent of inhibition determined in two sets of experiments versus the corresponding uninhibited release of product. Both plots demonstrate that the hydrolytic activity of Cel7A suffers as a result of mutations in the product binding site that alleviate product inhibition (the rightmost point in each case corresponds to the wild-type enzyme). Furthermore, the activity of Cel7A is more

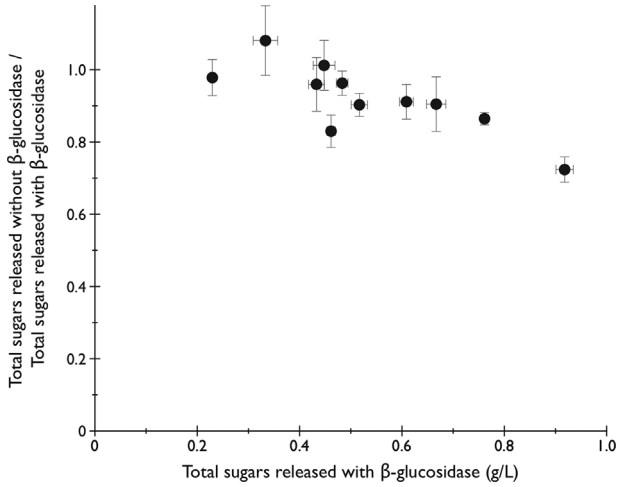

Figure 5. Scatterplot illustrating *Te*Cel7A variants' tolerances to inhibition by cellobiose compared to their uninhibited hydrolytic activities. Error bars represent propagated standard error (y) and standard error (x).

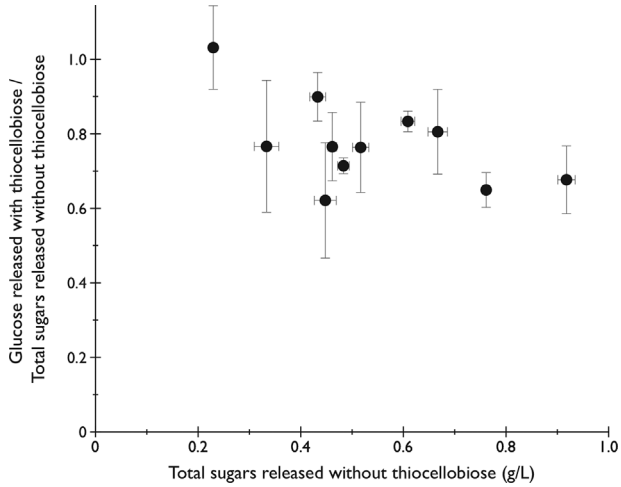

Figure 6. Scatterplot illustrating *Te*Cel7A variants' tolerances to inhibition by thiocellobiose compared to their uninhibited hydrolytic activities. (Note that "total sugars released without thiocellobiose" is equivalent to "total sugars released with β-glucosidase" and reactions with thiocellobiose included β-glucosidase.) Error bars represent propagated standard error (y) and standard error (x).

sensitive to such mutations than is the extent of inhibition. The uninhibited activity varies four-fold compared to just 1.5-fold for the extent of inhibition. It is also noteworthy that for some mutants, the effect of cellobiose on enzyme activity is negligible.

Conclusions

Inhibition of Cel7A is of particular relevance to the cellulosic biofuels industry, where high-solids loadings (leading to high cellobiose concentrations upon hydrolysis) are important for generating the concentrated glucose solutions necessary for downstream conversion to fuels and chemicals (Andrić et al., 2010). Under these conditions, product removal must be swift and efficient due to the adverse contribution of product inhibition to cellulose hydrolysis. As our experiments have demonstrated, alleviating product inhibition in Cel7A requires a delicate balance between maintaining affinity for cellobiose in the active site of the enzyme and allowing for its escape.

Our results experimentally validate computational predictions (Bu et al., 2011; Silveira and Skaf, 2015) for alleviating product inhibition in Cel7A; however, as hypothesized, they reveal a trade-off between catalytic efficiency and product tolerance. All ten *Te*Cel7A mutants examined displayed improved tolerances to cellobiose, with some exhibiting no inhibition; yet, large variations in activity were observed. Mutations of residue Y385, in particular, are of interest due to the demonstrated favorable affect on inhibition without a substantial loss in activity (achieved with an alanine substitution). Less drastic mutations of this amino acid, perhaps from tyrosine to phenylalanine, may yield similar product tolerance improvements (by conceivably preventing an electrostatic interaction with R248 obstructing cellobiose release, Fig. 4) at a minimal cost to catalytic activity. Future experiments exploring such options may result in a product-tolerant Cel7A mutant with catalytic activity comparable to that of the wild-type enzyme. Such an enzyme would improve the efficiency of cellulose hydrolysis and thereby lower the cost of the resulting biofuel, improving the likelihood of renewable energy adoption.

The authors thank Yuzhang Chen, Dr. Erin Imsand, Dr. Craig Dana, and Dr. Stefan Bauer for their contributions. This work was funded by the Energy Biosciences Institute.

References

Andrić P, Meyer AS, Jensen PA, Dam-Johansen K. 2010. Reactor design for minimizing product inhibition during enzymatic lignocellulose hydrolysis: I. Significance and mechanism of cellobiose and glucose inhibition on cellulolytic enzymes. Biotechnol Adv 28:308–324.

Becker D, Braet C, Brumer H, Claeyssens M, Divne C, Fagerström BR, Harris M, Jones TA, Kleywegt GJ, Koivula A, Mahdi S, Piens K, Sinnott ML, Ståhlberg J, Teeri TT, Underwood M, Wohlfahrt G. 2001. Engineering of a glycosidase Family 7 cellobiohydrolase to more alkaline pH optimum: the pH behaviour of *Trichoderma reesei* Cel7A and its E223S/ A224H/L225V/T226A/D262G mutant. Biochem J 356:19–30.

Bu L, Beckham GT, Shirts MR, Nimlos MR, Adney WS, Himmel ME, Crowley MF. 2011. Probing carbohydrate product expulsion from a processive cellulase with multiple absolute binding free energy methods. J Biol Chem 286:18161–18169.

Bu L, Nimlos MR, Shirts MR, Ståhlberg J, Himmel ME, Crowley MF, Beckham GT. 2012. Product binding varies dramatically between processive and non-processive cellulase enzymes. J Biol Chem 287:24807–24813.

Colussi F, Sørensen TH, Alasepp K, Kari J, Cruys-Bagger N, Windahl MS, Olsen JP, Borch K, Westh P. 2015. Probing substrate interactions in the active tunnel of a catalytically deficient cellobiohydrolase (Cel7). J Biol Chem 290: 2444–2454.

Dana CM, Dotson-Fagerstrom A, Roche CM, Kal SM, Chokhawala HA, Blanch HW, Clark DS. 2014. The importance of pyroglutamate in cellulase Cel7A. Biotechnol Bioeng 111:842–847.

Dana CM, Saija P, Kal SM, Bryan MB, Blanch HW, Clark DS. 2012. Biased clique shuffling reveals stabilizing mutations in cellulase Cel7A. Biotechnol Bioeng 109:2710–2719.

Daniel Gietz R, Woods RA. 2002. Transformation of yeast by lithium acetate/single-stranded carrier DNA/polyethylene glycol method. In: Guthrie C, Fink GR, editor. Methods Enzymol. Academic Press. Guide to Yeast Genetics and Molecular and Cell Biology - Part B, Vol. 350, pp. P 87–96.

Dinan T. 2014. The Renewable Fuel Standard: Issues for 2014 and Beyond. *Congr. Budg. Off.* https://www.cbo.gov/publication/45477.

Divne C, Ståhlberg J, Teeri TT, Jones TA. 1998. High-resolution crystal structures reveal how a cellulose chain is bound in the 50 Å long tunnel of cellobiohydrolase I from *Trichoderma reesei*. J Mol Biol 275: 309–325.

Fox JM, Levine SE, Clark DS, Blanch HW. 2011. Initial- and processive-cut products reveal cellobiohydrolase rate limitations and the role of companion enzymes. Biochemistry (Mosc.) 51:442–452.

Gericke M, Schlufter K, Liebert T, Heinze T, Budtova T. 2009. Rheological properties of cellulose/ionic liquid solutions: from dilute to concentrated states. Biomacromolecules 10:1188–1194.

Hanson SR, Stege JT, Cheng C, Luginbuhl P. 2014. Variant CBH I polypeptides with reduced product inhibition. US20140287471 A1. http://www.google.com/patents/ US20140287471.

Jalak J, Kurašin M, Teugjas H, Väljamäe P. 2012. Endo-exo synergism in cellulose hydrolysis revisited. J Biol Chem 287:28802–28815.

Klein-Marcuschamer D, Oleskowicz-Popiel P, Simmons BA, Blanch HW. 2012. The challenge of enzyme cost in the production of lignocellulosic biofuels. Biotechnol Bioeng 109:1083–1087.

Knott BC, Crowley MF, Himmel ME, Ståhlberg J, Beckham GT. 2014. Carbohydrate-protein interactions that drive processive polysaccharide translocation in enzymes revealed from a computational study of cellobiohydrolase processivity. J Am Chem Soc 136:8810–8819.

Kuusk S, Sørlie M, Väljamäe P. 2015. The predominant molecular state of bound enzyme determines the strength and type of product inhibition in the hydrolysis of recalcitrant polysaccharides by processive enzymes. J Biol Chem 290:11678–11691.

Labbé S, Thiele DJ. 1999. [8] Copper ion inducible and repressible promoter systems in yeast. Methods Enzymol 306:145–153.

Mulakala C, Reilly PJ. 2005. *Hypocrea jecorina* (*Trichoderma reesei*) Cel7A as a molecular machine: a docking study. Proteins 60:598–605.

Murphy L, Bohlin C, Baumann MJ, Olsen SN, Sørensen TH, Anderson L, Borch K, Westh P. 2013. Product inhibition of five *Hypocrea jecorina* cellulases. Enzyme Microb Technol. 52:163–169.

Nakamura A, Tsukada T, Auer S, Furuta T, Wada M, Koivula A, Igarashi K, Samejima M. 2013. The tryptophan residue at the active site tunnel entrance of Trichoderma reesei cellobiohydrolase cel7a is important for initiation of degradation of crystalline cellulose. J Biol Chem 288:13503–13510.

Payne CM, Jiang W, Shirts MR, Himmel ME, Crowley MF, Beckham GT. 2013. Glycoside hydrolase processivity is directly related to oligosaccharide binding free energy. J Am Chem Soc 135:18831–18839.

Payne CM, Knott BC, Mayes HB, Hansson H, Himmel ME, Sandgren M, Ståhlberg J, Beckham GT. 2015. Fungal cellulases. Chem Rev 115:1308–1448.

Silveira RL, Skaf MS. 2015. Molecular dynamics simulations of family 7 cellobiohydrolase mutants aimed at reducing product inhibition. J Phys Chem B 119(29):9295–9303 http://dx.doi.org/10.1021/jp509911m

Somerville C, Bauer S, Brininstool G, Facette M, Hamann T, Milne J, Osborne E, Paredez A, Persson S, Raab T, Vorwerk S, Youngs H. 2004. Toward a systems approach to understanding plant cell walls. Science 306:2206–2211.

Teugjas H, Väljamäe P. 2013. Product inhibition of cellulases studied with C-14-labeled cellulose substrates. Biotechnol Biofuels 6:104.

Supporting Information

Additional supporting information may be found in the online version of this article at the publisher's web-site.